IMPROVEMENT OF FLEXURAL BOND STRENGTH OF ZIRCONA-RESIN CEMENT BY SURFACE PATTERNING USING SUB-NANOSECOND UV LASER

Canan Akay[1] Neslihan Turan[2] Duygu Karakıs[3] Luis Alberto Angurel[4]

[1]Department of Prosthodontics, Faculty of Dentistry, Osmangazi University, Eskişehir, Turkey
[2]Department of Physics, Faculty of Science, Gazi University, Ankara, Turkey
[3]Department of Prosthodontics, Faculty of Dentistry, Gazi University, Ankara, Turkey
[4]Instituto de Ciencia de Materiales de Aragón, ICMA, CSIC-Universidad de Zaragoza

Abstract

Zirconia is a dental material that shows excellent biocompatibility and high strength in clinical applications. This study aims to evaluate the effects of ultrafast laser applications. The surface nanostructures were classified into three groups. Group 1 was generated using the burst mode, with three different distances between dots: 52 μm (Group 1a), 104 μm (Group 1b), and 156 μm (Group 1c). Group 2 was processed using the scanning mode configuration, with a set of parallel lines. Group 3 was also processed using this scanning configuration creating a set of square-shaped patterning. Group 4 was the control group. After the surface treatments, a pair of zirconia specimens was bonded end to end with resin cement. Flexural bond strength (FBS) test was applied in a universal test machine. Multiple comparisons were performed using a one-way analysis of variance and the Tukey's HSD test. All the samples that were treated with the laser showed higher FBS values than the untreated surface. Using the burst mode, preformed circular-shaped surface on an angle of 90^0 at 52 μm distance (Group 1a) showed the highest FBS values among all groups ($p < .05$). Groups 2 and 3 had significantly higher values than 1b and 1c.

Key words: dental material, Y-TZP, zirconia, surface treatment, UV lasers, four point bending test

1. Introduction

All-ceramic dental restorations using yttrium-stabilized tetragonal zirconia polycrystal (Y-TZP) materials are the cutting-edge solutions, about esthetic advantage as well as mechanical durability.[1] The most important mechanical advantage of Y-TZP ceramics is their resistance to crack propagation, which can be traced to the crystal conversion effect. Shear stress in the Y-TZP ceramic particles resulting from a beginning crack causes a transformation from the tetragonal to the monoclinic phase. As this transformation leads to a volume expansion by 3%–5%, it closes the crack, increasing the energy threshold for further growth of the crack and thus inhibits a further crack opening.[2,3] Despite Y-TZP ceramics are widely used in dentistry, there is not yet an optimum bonding protocol between ceramic surfaces and dental structures.[4] Conventional types of cement provide adequate adhesion for zirconia restorations;[5,6,7] however in many applications such as short or tapered prepared tooth structures, sufficient bond strength is important for high retention, prevention of microleakage, and increased fracture/fatigue resistance. In consequence, bonding techniques require to be optimized.[8] Under appropriate conditions, resin cement provides higher bonding strength with better mechanical properties than conventional cement.[5,6,7] It is based on a strong resin bond, surface roughening, and micromechanical locking created by chemical adhesion between cement and ceramic.[8] Many surface roughening methods have been tried in recent years, including hydrofluoric acid etching after fused glass-ceramic application, selective infiltration etching, roughening the surface with diamond rotary systems, airborne-particle-abrasion, surface fluorination, nano-alumina coating, silica coating, hot chemical etching, laser irradiation, or combination of this methods.[9] However, physical changes related to the surface modifications such as external stresses, grinding pressure, and thermal stresses can lead to phase transformation[10] and reduce the flexural strength.[11]

Laser usage has become widespread recently in medicine and dentistry. Laser processes are contactless and wear-free.[12] Therefore they can result in clean procedures without the use of chemicals and contamination.[13] Several laser treatments on zirconia surfaces have been carried out using Er-YAG (erbium-doped yttrium aluminum garnet), Nd: YAG (neodymium-doped yttrium aluminum garnet), and CO_2(carbon dioxide) lasers for surface roughening, and these have been demonstrated to be useful alternatives to conventional surface roughening techniques.[14] However it has been stated that thermal laser processes, usually observed when long pulse (>ns) lasers are used, may lead to melting, generating a heat-damaged layer, loss of surface material and deep cracks.[15,16] The appearance of new ultrashort lasers opens new possibilities due to the short pulse width values, lower and more localized thermal effects. Also, due to the high irradiance values, new nonlinear processes can be generated. As a relatively new technology, ultrashort lasers have begun to be used to micromachine zirconia ceramic surfaces.[14] Ultrafast lasers ablate Y-TZP despite their low absorption for most laser wavelengths, as the large irradiances of focused laser pulses initiate the generation of free electrons at the ceramic surface. This technique can generate ablation very precisely on ceramic surfaces and avoid thermal effects that could otherwise cause phase transformations and reduce the sample strength.[12] Many studies have shown that ultrashort laser technology can provide a gentle, precise, and clear surface without heating.[10,17,18] A recent study by Kara et al also showed that ultrashort (femtosecond) laser application is an effective method for control the roughness of zirconia ceramics, increasing the bond strength between zirconia and resin cement.[19]

Also, the ablation process is located in a thin surface layer without exhibiting phase transformation and disturbing the material properties.[20]

Laser technologies are evolving very fast and new opportunities are opening to apply them not only in planar samples but also in samples with complex geometries. Combining laser beams with high quality, different optical configurations, and the possibilities of combining the control of the laser with 5- or 7-axis machines, it is possible to define protocols to machine samples with very different 3D shapes.[21,22] Also an adequate combination of focusing lenses allows to machining the inner surface of pieces with complex shapes, for instance, calibers with high aspect ratios.[23]

Data obtained from the clinic regarding the survival rates of all-ceramic materials reveal that their restoration is susceptible to breakage due to repeated occlusal loading.[24,25,26] For this reason, the in vitro characterization of dental ceramics should include a test method capable of accessing their fracture properties.[27] The survival time of all-ceramic systems is strongly related to the flexural strength of the restoration, which is the result of the FBS between zirconia and resin.[28] Flexural strength is generally considered a meaningful and reliable characterization parameter to assess the ceramics, as their properties are weaker in tension than compression.[29,30]

Several test methods have been introduced to measure the mechanical strength of brittle ceramic materials. Considering that the bond-force test should use a system that correctly pushes the adhesive interface, but that the shift represents several inaccuracy modes, yet this information has not yet been shown in practice. Nevertheless, there are several problems, including shear tests, homogeneity of stress area, and obvious stress concentrations and parasitic stresses. On the contrary, the interface tension is said to be preferable. However, there are difficulties in the preparation, alignment, and fixation of samples of direct stress. At the same time, there is a tendency for non-homogeneous stress distribution. Flexural strength tests, on the contrary, are relatively easy to install and are prevented from sample fixation problems. Among them, flexure three-point bending and four-point tests are the most common. Beam shaped samples, with a rectangular cross-section, are supported in two points and the load is applied vertically at either one point (three-point flexure test) or two points (four-point flexure test).[26] In the first case, a nonuniform stress field is created under the loading piston, whereas in the second case the stress field between the support rolls is uniform. The problem with brittle ceramics materials is that inherent material inhomogeneity can induce flaws such as microcracks or grain pullouts throughout the volume or on the surface of a material.[28] Therefore, uniform vertical load applied by four-point bending test can evaluate the stress for the entire beam sample, even for a joint system, with a high sensitivity."

Although many studies have reported the advantages of ultrafast laser ablation processes, there is no standard protocol for making the treatments. To perform this optimization, it is important to systematically characterize the effects of different laser parameters regarding irradiation of laser pulses, cutting speeds, and handling of the workpiece on the quality of roughened shapes of Y-TZP zirconia. In the present study, we have explored the possibility of using subnanosecond pulsed UV lasers on the FBS of Y-TZP and resin cement junctions. These lasers are cheaper than femtosecond ones and the use of UV radiation produce on the surface of material different effects than then-IR lasers. The purpose of the present study was to evaluate the effect of three different geometries of laser-induced microstructures on the surface of the Y-TZP generated with different configurations.

2. Material and Methods

A total of 25 pairs of rectangular prism zirconia samples (25 mm ± 0.4 mm) x (5 mm ± 0.4 mm) x (2 mm ± 0.4 mm) were used in this study. The specimens were milled from presintered zirconia blocks (ICE Zirkon, Zirkonzahn, Bruneck, Italy) by using Zirkograph 025 ECO (Zirkonzahn, Bruneck, Italy). The specimens were sintered at 1500ºC for 8 h in a high temperature sintering furnace for zirconia (Zirkonofen 600/V2, Zirkonzahn, Bruneck, Italy). The sample geometry was defined according to previously published four-point bending experiments.[9] To achieve surface standardization in zirconia samples, the samples were polished with 600-, 800-, 1000- and 1200 grit rotating silicon carbide abrasives (3M) in an automatic water polishing machine (Esetron). Before the laser surface treatment, the samples were cleaned in ultrasounds for 15 min with 96% ethanol and 15 min with distilled water to remove any particulate residue. Samples were then air-dried.

2.1. The subnanosecond-UV laser irradition process

A UV pulsed laser (λ = 355nm) (Rofin-Sinar) was used to modify the Y-TZP surface roughness at ICMA (CSIC-University of Zaragoza, Zaragoza Spain). Pulse width is 300 ps and in the experiments presented in this work, a frequency of 400 kHz and an average power of 2.03 W were used. The diameter of the laser beam is approximately 32 μm. The laser is coupled to a galvanometric mirror allowing scanning the surface of the sample. With these laser parameters; the fluence value of a spot is estimated to be 0.63 J/cm^2 and the spot irradiance 2.10 GW/cm^2. Y-TZP surfaces were treated in the burst or the scanning mode. In all the cases, the samples are placed perpendicular (90º) to the laser incidence plane. Depending on the laser configuration, three different types of geometries have been generated in the Y-TZP surfaces. This fact allows dividing the samples into three groups:

Group 1; Using the burst mode, a set of circular-shaped holes distributed on the surface in a square lattice was performed with different lattice parameters: 52 μm (Group 1a), 104 μm (Group 1b), and 156 μm (Group 1c). In each position, the number of bursts is 300.

Group 2; Using the scanning mode, a line-shaped pattern was obtained, leaving a distance between lines of 52 μm. The laser scanning velocity was 200 mm/s and the scanning was performed in the direction parallel to the laser beam polarization direction, perpendicular to the 5 mm edge of the sample.

Group 3; Using the scanning mode, a square-shaped pattern was fabricated, in the directions parallel and perpendicular to the polarization direction. Also, in this case, the lattice parameter is 52 μm and the scanning velocity was 200 mm/s.

Group 4 (Control Group): No surface treatment was applied to the zirconia ceramic surfaces of these samples.

A confocal microscope (Model 2300 PLμ, Sensofar, Spain), with a x100 objective, was used to measure the topography of one sample from each group.

2.2. Cementation procedure

Surface laser treatments were applied to 5 mm x 2 mm surface areas of zirconia samples. After the surface treatments, a pair of zirconia specimens was bonded end to end with resin cement. Resin cement thickness was set to 0.1 mm to create a standard cementation surface. A special stainless steel mold was used to keep this

thickness at a standard value. Resin cement was mixed according to the manufacturer's recommendations. The catalyst paste and the base paste were mixed for 20 s using a spatula to form a homogeneous mixture. During the mixing process, care was taken not to create air bubbles. Zirconia samples were placed in the mold. Resin cement (Panavia SA Cement Plus, Kuraray), with the components presented in Table 1 was applied to the 5mm x 2 mm surfaces of the samples by using sponge pellet. Excess cement residues were removed before polymerization. The zirconia samples were then light polymerized without moving for 20 s from the two opposite sides (Blue Lex LD-105, Monitex Industrial Co.). The samples were maintained in a fixed position for 5 min without any movement to ensure self-polymerization.

Table 1. Experimental materials and their characteristics

Product Batch	Composition	Manufacturer	Lot Number
Zirconia	ZrO_2; specifications, Y_2O_3 % 4-6, Al_2O_3 % 1, SiO_2 % max. 0.02, Fe_2O_3 % max. 0.01, Na_2O % max. 0.04	Zirkon-Zahn, Bruneck, Italy	ZB3056B
Panavia SA Cement Plus	Paste A: MDP/Bis GMA/ TEGDMA/HEMA Hydrophobic aromatic dimethacrylate Silaned barium glass filler, silaned colloidal silica, dl-Camphorquinone, peroxide, catalysts, pigments Paste B: Hydrophobic aromatic dimethacrylate, Hydrophobic aliphatic dimethacrylate, silaned barium glass filler, surface treated sodium flouride, accelerators, pigments	Kuraray Noritake Dental Inc., Okayama, Japan	4L0041

Abbreviations: Bis-GMA, Bisphenol A glycol dimethacrylate; HEMA, 2-hydroxyethyl methacrylate; MDP, 10-Metacryloxydecyl dihydrogen phosphate; TEGDMA, Triethylene glycol dimethacrylate.

2.3. Four-point bending test

The adhesion interface of the zirconia samples bonded with end-to-end resin cement is centrally assembled between the upper load points (Figure 1). The distance between the centers of the supporting rollers was 40.0 mm and the distance between the centers of the loading rollers was adjusted to 20.0 mm. The load was applied on a universal test machine (Lloyd-LRX, Lloyd Instruments) with a 2.0-mm radius rods and with a cross speed of 1 mm/min until the bonding failure occurred (Figure 1).

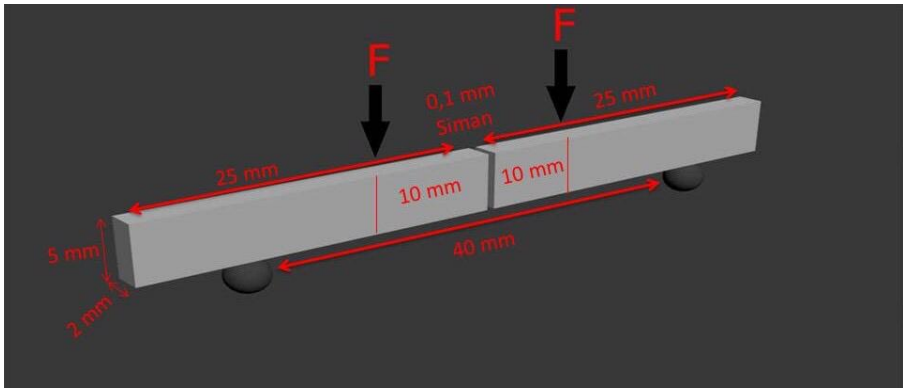

Figure 1: Shematic view of the 4-point bending test

2.4.Statistical analysis:

FBS was analyzed with statistical software (SPSS 16.0,Chicago, IL). The normality of the distribution of data was examined using Kolmogorov-Smirnov Test ($\alpha = 0.05$) (Table 2) One-way ANOVA was used to analyze the data for significant differences. (Table 3) The Tukey HSD test was performed for multiple comparison. The significance level was set at $p < 0.05$.

Table 2. Kolgomorov-Smirnov test restults

One-Sample Kolmogorov-Smirnov Test							
		Group1a	Group1b	Group1c	Group2	Group3	Control
N		5	5	5	5	5	5
Normal Parameters (a,b)	Mean	34.04954	23.87421	23.24048	27.66253	26.25817	16.01556
	Std. Deviation	0.479468	0.413747	0.297066	1.166934	2.094621	5.47192
Most Extrem Differences	Absolute	0.219857	0.219857	0.219857	0.219857	0.219857	0.144286
	Positive	0.219857	0.219857	0.219857	0.139508	0.139508	0.144286
	Negative	-0.13951	-0.13951	-0.13951	-0.21986	-0.21986	-0.10319
Kolmogorov-Smirnov Z		0.491615	0.491615	0.491615	0.491615	0.491615	0.612154
Asymp.Sig. (two-tailed)		0.969056	0.969056	0.969056	0.969056	0.969056	0.847792
A	Test distribution is Normal						
B	Calculated from data						

TABLE 3 Statistical results of flexural bond strength value of the groups according to One-way ANOVA analysis

		Mean Difference (I-J)	**Std. Error**	**Sig.**	**95% Confidence Interval**	
		Lower bound	**Upper bound**	**Lower bound**	**Upper bound**	**Lower bound**
Group 1a	1b	10, 17, 533 (*)	,70,646	,000	8,0613	12,2893
	1c	10,80,906*)	,70,646	,000	8,6951	12,9230
	2	6,38,701*)	,70,646	,000	4,2730	8,5010
	3	7,79,137 (*)	,70,646	,000	5,6774	9,9054
Group 1b	1a	-10,17,533 (*)	,70,646	,000	-12,2893	-8,0613
	1c	,63,373	,70,646	,895	-1,4802	2,7477
	2	-3,78,832 (*)	,70,646	,000	-5,9023	-1,6743
	3	-2,38,398 (*)	,70,646	,022	-4,4979	-,2700
Group 1c	1a	-10,80,906 (*)	,70,646	,000	-12,9230	-8,6951
	1b	-,63,373	,70,646	,895	-2,7477	1,4802
	2	-4,42,205 (*)	,70,646	,000	-6,5360	-2,3081
	3	-3,01,769 (*)	,70,646	,003	-5,1317	-,9037
Group 2	1a	-6,38,701 (*)	,70,646	,000	-8,5010	-4,2730
	1b	3,78,832 (*)	,70,646	,000	1,6743	5,9023
	1c	4,42,205 (*)	,70,646	,000	2,3081	6,5360

	3	1,40,437	,70,646	,307	-,7096	3,5183
Group 3	1a	-7,79,137 (*)	,70,646	,000	-9,9054	-5,6774
	1b	2,38,395 (*)	,70,646	,022	,2700	4,4979
	1c	3,01,769 (*)	,70,646	,003	,9037	5,1317
	2	-1,40,437	,70,646	,307	-3,5183	,7096

3. Results:

Using confocal microscopy, we have performed an analysis of the topography of the surface in the different groups of laser-treated samples and the results are presented in Figures 2, 3, and 4. Figure 2 is focused on samples of group 1, where a burst configuration has been used to uniformly distribute a set of circular holes around the sample. Figure 2A shows the distribution of holes in the sample that has been processed with a distance of 52 µm between holes. In the other subgroups distance between holes is higher and only one hole is observed in the images.

The topography of the samples with a linear patterning is presented in Figure 3. Taking into account the scanning speed and the frequency, the distance between two consecutive dots is 0.5 µm, and in consequence an overlapping of 98.5% was used during laser processing.

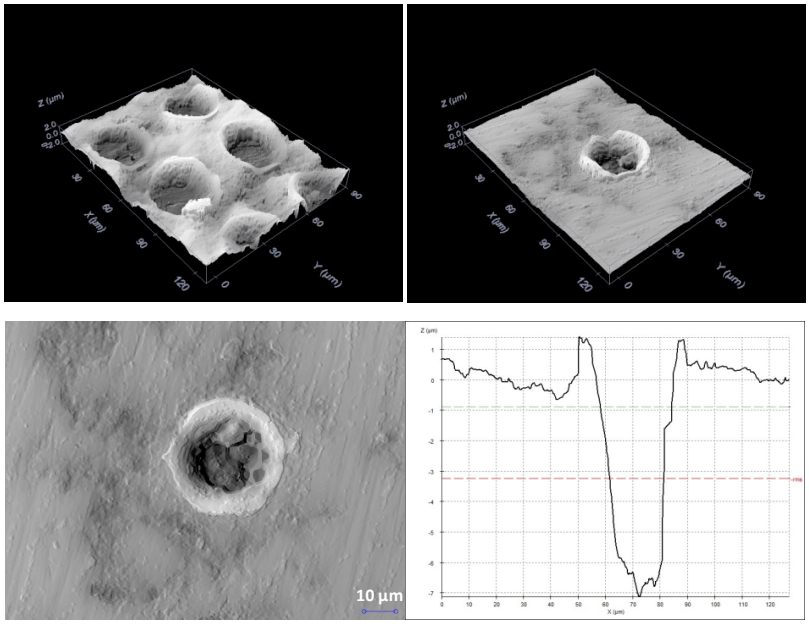

Figure 2: Topography of the microstructures generated in group 1 samples: (a) 3D image in the case of a distance of 52 µm between dots (subgroup 1a), (b) 3D image of one hole in the case of the sample of subgroup 1b (104 µm between dots), (c) 2D representation of the topography in this sample, (d) linear profile along the center of the hole.

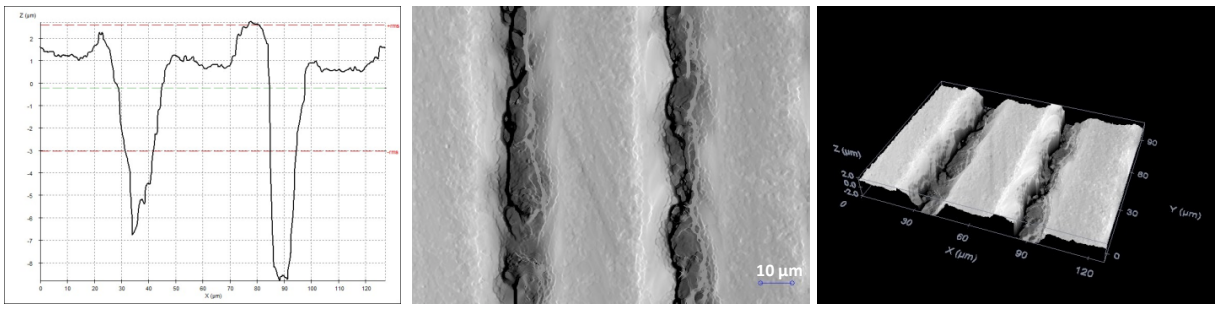

(I) (II) (III)

Figure 3: Topography of the microstructures generated in group 2 samples with a linear configuration: (a) 3D image, (b) 2D representation of the topography in this sample, (c) linear profile perpendicular to the lines.

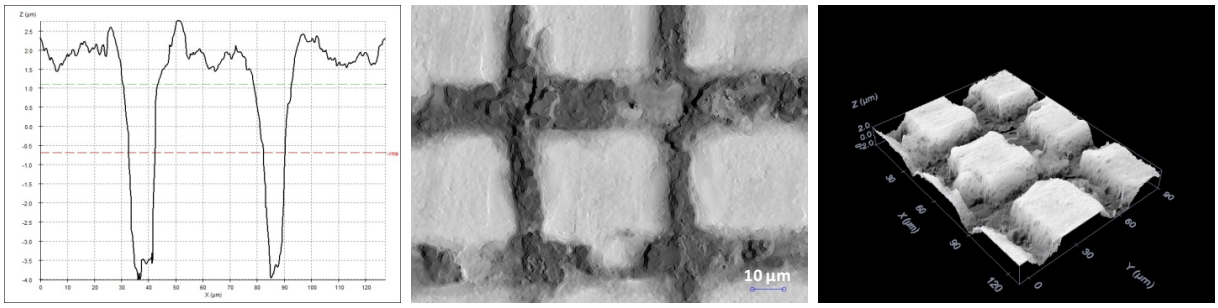

(I) (II) (III)

Figure 4: Topography of the microstructures generated in samples of group 3 with a square configuration: (a) 3D image, (b) 2D representation of the topography in this sample, (c) linear profile perpendicular to the lines.

Figure 4 shows the topography of samples of group 3, with a square-like patterning. Since the laser beam is elliptical, the widths of the horizontal and vertical lines are different.

The mean and standard deviations of FBS values measured in the five different groups (Group 1 (a,b,c), Group 2, Group 3) are listed in Table 4. Results show that the FBS values are higher in all the samples after laser micro-structuring in comparison with the untreated surfaces (Control group = 15.31 N) ($p < 0.05$). Statistical analysis indicated that FBS is affected by the roughness of surface patterns. The Tukey's HSD test showed that Group 1a (burst mode with the shortest distance between dots, 52 µm) showed the highest FBS values among all groups ($p < 0.05$). Groups 2 and 3 show significantly higher values than 1b and 1c but did not reveal statistically significant differences from each other ($p < 0.05$). Similarly, Group 1b (104 µm distance between dots in burst mode) and 1c (156 µm distance in burst mode) did not show statistically significant values from each other ($p > 0.05$).

TABLE 4 Mean values of flexural bond strength test (in MPa)

Groups (n = 5)	Mean (MPa)	Standard Deviation	Deformated surface area (%)
Group 1a	$34.04^{a,b,c,B,C}$	0.47	26
Group 1b	$23.87^{b,d}$	0.41	7
Group 1c	$23.24^{c,e}$	0.29	3
Group 2	$27.66^{A,B}$	1.16	46
Group 3	$26.25^{C,D}$	2.09	71
Group 4 (Control)	$5.31^{a,d,e,A,D}$	5.25	-

*Same superscript lower case letters describe statistical differences in flexural bond strength test in Group 1a,1b,1c and Group 4 (Control group). Same superscript upper case letters describe statistical differences in flexural bond strength in Group 1a, 2 ,3, and 4 (Control group) ($\alpha = 0.05$).

4. Discussion

Zirconia surface treatment is a challenging task when applying adhesive cementation. This requires an alternative surface modification method that can improve the surface properties and increase the bond strength. Several methods have been purposed to overcome this challenge.[31] Here the study evaluated the effects of ultrafast laser, and all laser-treated samples showed higher bending strength values than the untreated surface. Using the burst mode, a circular-shaped Surface was made at an angle of 900 µm (Group 1a) at an angle of 900 µm ($p < 0.05$)) showing the highest FBS values among all groups. Groups 2 and 3 had significantly higher values than 1b and 1c.

Considering that the bond-force test should use a system that correctly pushes the adhesive interface, it is determined that the shift represents several inaccuracy modes, yet this information has not yet been shown in practice. Nevertheless, there are some problems, including shear tests, homogeneity of stress area and obvious stress concentrations and parasitic stresses. On the contrary, the interface tension is said to be preferable. However, there are difficulties in the preparation, alignment, and fixation of samples of direct stress. At the same time, there is a tendency for nonhomogeneous stress distribution. Flexural strength tests, on the contrary, are relatively easy to install and are prevented from sample fixation problems.

Four-point bending test shows a higher consistency than the tensile bond test in evaluating the bond strengths.[32] In microtensile tests, the different behaviors of the materials interact as the resin, machined surfaces and zirconia have different elastic moduli, Poisson's ratios, and forces. A pure, uniform tension field cannot be obtained. This situation cannot be controlled. In the usual so-called “shear tests,” uncontrolled and unmeasurable parasitic stresses occur because the bending of the material cannot be prevented despite all the precautions taken in test designs. In contrast, three-point bending and microtensile tests are recommended for homogeneous materials, while four-point bending tests should be preferred where appropriate for heterogeneous materials.[9,33]

The surface characteristics of ceramics have a major influence on the quality of the contact between the adhesive and the solid ceramic surface. The adhesive wets and spreads over the surface, penetrating pits of roughened surfaces.[34] The success of resin bonding relies on the mechanical bonding through the micromechanical interlocking of the roughened surfaces. Phosphoric acid (H_3PO_4) or hydrofluoric acid (HF) etching are commonly recommended methods used to roughen the surface of silica-based ceramics, however, unfortunately, H_3PO_4 and HF cannot be used effectively on ZrO_2, making it difficult to roughen the surface for mechanical retention.[8,35] Also, the lack of silica in Y-TZP zirconia inhibits the chemical bonding with silanization. Therefore, because of the difficulty in creating mechanical and chemical bonding in ZrO_2, alternative methods have been explored to bond ZrO_2 using resins. Surface grinding with 50 μm size Al_2O_3 is commonly used for roughening the surface of ZrO_2 to improve mechanical bonding. However, research has shown that these techniques can create surface microcracks that can decrease strength and apparent fracture toughness. Surface grinding also generates a tetragonal to monoclinic phase change on the surface of zirconia.[36-37]

In recent years, the use of ultrafast lasers in the dentistry industry has increased. Previous investigations have shown that ultrafast laser pulses can be used to surface treatment process of zirconia ceramics with high precision and low loss in flexural strength.[38] This technique can ablate material in the thin surface layer without exhibiting phase transformation and disturbing the material properties.[20] It has been shown that for the microstructuring of densely sintered Y-TZP, ultrafast pulsed lasers are a suitable tool. [38]

However, systematic research to evaluate the influence of different patterns geometries generated with sub-nanosecond UV lasers on FBS between zirconia-resin cement has not been performed previously. In the present study, we have evaluated three different laser irradiation protocols. According to the results obtained in this study, it can be concluded that the different laser patterning configurations strongly influence the FBS values on Y-TZP-resin cement junctions. All treated surfaces were roughened and revealed significantly higher FBS values than in samples without laser treatment. Surface roughness plays an important role in the FBS of the surface and increases the surface wettability.[39,40]

On comparing the three surface patterns analyzed in the present study, circular-shaped treated surfaces with a low distance between holes (Group 1a, 34,04 MPa) obtained using a burst configuration, showed the highest

FBS values. In many previous studies, it has been showing that an increase in surface roughness leads to higher FBS values and that increase in surface roughness also strengthened the connection between resin cement and zirconia.[36] However, in the present study, we have observed that the best results have not been obtained on the surfaces with the highest roughness values. Samples of Groups 1a, 1b, 2, and 3 have higher roughness values than samples of Group 1a and the values of FBS are approximately 23%–46% higher in this set of samples. From the information obtained from confocal microscope images, surface pattern in Group 1a was seen in the circular-shape with the equal distance (52 μm) from each other. According to the analysis of confocal profile images, the deformation width of surface patterns of treated samples was 6.36, 5.53, and 5.41 μm for Group 1, 2, and 3 respectively. On comparison of surface patterns treated with ps-UV laser, the highest FBS value of Group 1 could be related to the deformation width of treated surfaces. On the other hand, although the ablation with the ultrafast lasers is known to minimize the thermal effect, debris agglomeration and solidification in the surface of Y-TZP material is an issue for the ablation of Y-TZP with line overlaps.[38] In the scanning mode that performed line-shaped pattern over a point there are 69 dots, however, in burst scanning mode there have only been 300 dots. In the case of burst configurations (Group 1), molten material agglomerates in an outer crown in the border of the hole (Figure 2) producing a nearly uniform distribution in the entire surface. In the line scanning geometries (Groups 2 and 3), the molten material is deposited again in areas that have been machined producing some debris agglomerations that generate some defects in the machined regions (Figures 3 and 4), reducing the effectiveness of the pattern for increasing FBS.

Yücel *et al* evaluated the shear bond strength (SBS) of square-, spiral-, and circular-shaped surface treatments using a femtosecond laser and modifying the angle of the sample - 30º and 90º.[39] Although there are different application protocols, the surface pattern of the treated surface with 90º laser beam angle showed similar behavior to those obtained with the burst and square-shaped surface patterns used in the present study. Yücel *et al* found that surface roughness and SBS values of the square and spiral pattern configurations (12.5 MPa and 12.3 MPa, respectively) were higher than in circular shape (6.57 MPa) surface.[39] The increase in surface roughness also strengthened the connection between resin cement and zirconia. Also, stronger laser treatments, as in the case of Group 2 and 3 could give rise to higher heat generation that could lead to microcrack propagation. Therefore, the lower FBS values in the square-shaped surface pattern analyzed in the present study could be related to a higher heat generation of square-shaped surfaces that lead to reduced mechanical properties.

In a comparison of three different distances of the circular-shaped surface patterns (Group 1a,1b,1c), strong improvement of FBS values has been observed with an increase in the distance between dots. Expectedly, with increasing distance, the deformation rate of the samples was decreased, therefore increased deformation rate could be related to the increased FBS value.

As a summary, the increased surface deformation rate (or surface roughness) is not the only factor that determines the FBS values between Y-TZP resin cement; but also the pattern of the surfaces plays an important role. The FBS values of circular-shaped Y-TZP surface pattern are greater than that of the line-shaped and squared-line shaped Y-TZP surfaces. The present study has claimed that due to the possibility of debris agglomeration and more heat release related to pulse overlap in line-shaped (Group 2) and square-shaped (Group 3) Y-TZP surface, circular-shaped Y-TZP surface (Group 1) formed by burst mode with the highest FBS values have been suggested. The FBS value of circular-shaped Y-TZP surface in the 52μm distance was higher than 104μm and 152 μm distance.

This study also shows that subnanosecond pulsed UV lasers are adequate to machine Y-TZP ceramics and provides the desired surface form that may connect the resin cement systematically. Further studies are needed to optimize laser parameters to define processing protocols that improve the FBS of Y-TZP ceramics in dentistry. Artificial aging methods were not applied in the study which can be considered as one of the limitations of this study. Future studies should include thermal cycling and long-term water storage to evaluate FBS of resin-zirconia with different primers. Another limitation of this study is the small sample size (five beams for each group) that might induce the bias of the outcome. More studies are necessary.

5. Conclusion

The use of subnanosecond pulsed UV lasers can provide clinically acceptable FBS of zirconia ceramics and resin cement. These lasers are cheaper than femtosecond ones and the use of UV radiation produce on the surface of material different effects than then-IR lasers.

Acknowledgements

The authors thank the Spanish MINECO, Agencia Estatal de Investigación and the European FEDER Program (project ENE2017-83669-C4-1-R), and the Gobierno de Aragón "Construyendo Europa desde Aragón" (research group T54_17R). The authors declare that the article sent is original and no part of it has been published before or is being considered for the publication in any other journal. The authors declare that they do not have any financial interest in the companies whose materials are included in this article.

References

1. Barsch N, Barcıkowskı S, Baıer K. Ultrafast-laser-processed zirconia and its adhesion to dental cement. J Las Micro/Nanoengineering. 2008;3(2):78–83.
2. Weigl P, Kasenbacher A, Werelius K. Dental applications. In: F. Dausinger, F Lichtner, H Lubatschowski (Eds.). Femtosecond technology for technical and medical applications, Springer Topics in Appl. Phys. 2004; 96, 167.
3. Ardlin BI. Transformation-toughened zirconia for dental inlays, crowns, and bridges: chemical stability and effect of low-temperature aging on flexural strength and surface structure. Dent Mat. 2002;18:590.
4. Dias de Souza GM, Thompson VP, Braga RR. Effect of metal primers on micro-tensile bond strength between zirconia and resin cement. J Prosthet Dent. 2011;105:296–303.
5. Komine F, Tomic M, Gerds T, Strub J. Influence of different adhesive resin cement on the fracture strength of aluminum oxide ceramic posterior crowns. J Prosthet Dent. 2004; 92:359–64.
6. Matinlinna JP, Heikkinen T, Ozcan M, Lassila LV, Vallittu PK. Evaluation of resin adhesion to zirconia ceramic using some organosilanes. Dent Mater. 2006;22:824–31.
7. Menani LR, Farhat IA, Tiossi R, Ribeiro RF, Guastaldi AC. Effect of surface treatment on the bond strength between yttria partially stabilized zirconia ceramics and resin cement. J Prosthet Dent. 2014;112:357–64.
8. Thompson JY, Stoner BR, Piascik JR, Smith R. Adhesion/cementation to zirconia and other non-silicate ceramics: where are we now? Dent Mater. 2011;27(1):71–82.
9. Akay C, Tanış M., Mumcu E, Kılı.arslan MA, Şen M. Influence of nano alumina coating on the flexural bond strength between zirconia and resin cement. J Adv Prosthodont. 2018;10(1):43–9.

10. Akpinar YZ, Yavuz T, Aslan MA, Kepceoglu A, Kilic HS. Effect of different surface shapes formed by femtosecond laser on zirconia-resin cement shear bond strength. J Adhes Sci Technol. 2015;29(3):149–57.
11. Zhang Y, Lawn BR, Rekow ED, Thompson VP. Effect of sandblasting on the long-term performance of dental ceramic. J Biomed Mater Res B Appl Biomater. 2004;71:381–6.
12. Bärsch N, Gattı A, Barcıkowskı S. Improving laser ablation of zirconia by liquid films: multiple influence of liquids on surface machining and nanoparticle generation. J Las Micro/Nanoengineering. 2009;4(1):66–70.
13. Ji L, Li L, Devlin H, Liu Z, Jiao J, Whitehead D. Ti: sapphire femtosecond laser ablation of dental enamel, dentine, and cementum. Lasers Med Sci. 2012;27(1):197–204.
14. Erdur EA, Basciftci FA. Effect of Ti: sapphire laser on shear bond strength of orthodontic brackets to ceramic surfaces. Lasers Surg Med. 2015;47(6):512–9.
15. Foxton RM, Cavalcanti AN, Nakajima M, Pilecki P, Sherriff M, Melo L, et al. Durability of resin cement bond to aluminum oxide and zirconia ceramics after air abrasion and laser treatment. J. Prosthodont. 2011;20:84–9.
16. Erdem A, Akar G, Erdem A, Kose T. Effects of different surface treatments on bond strength between resin cement and zirconia ceramics. Oper Dent. 2014;39:118–27.
17. Fiedler S, Irsig R, Tiggesbaumker J, Schuster C, Merschjann C, Rothe N, et al. Machining of biocompatible ceramics with femtosecond laser pulses. Biomed Tech. (Berl.). 2013;58:4093.
18. Symietz C, Lehmann E, Gildenhaar R, Krüger J, Berger G. Femtosecond laser induced fixation of calcium alkali phosphate ceramics on titanium-alloy bone implant material. Acta Biomater. 2010;6:3318–24.
19. Kara O, Kara HB, Tobi ES, Ozturk AN, Kilic HS. Effect of various layers on the bond strength of two zirconia ceramics. Photomed Laser Surg. 2015;33(2):69–76.
20. Rethfeld B, Sokolowski-Tinten K, von der Linde D, Anisimov SI. Time scales in the response of materials to femtosecond laser excitation. Appl Phys A. 2004;79:767–9.
21. Ackerl N, Warhanek M, Gysel J, Wegener K. Ultrashort-pulsed laser machining of dental ceramic implants. J Eur Ceram Soc.m 2019;39:1635–41.
22. Kramer T, Remund S, Gafner M, Zwygart D, Neuenschwander B, Holtz R, et al. Novel strategy for ultrafast pulsed laser micromachining of rotational symmetric metallic parts. Procedia CIRP. 2018;74:611–7.
23. Zhan XP, Wang YJ, Su Y, Li MT, Zang HW, Xia H, et al. Micronano-texturing inner surfaces of small-caliber-high aspect ratio and super hydrophobic artificial vesselsusing femptosecond laser filament pulses. Adv Mat Interfaces. 2018;5:1801148.
24. Zhang Y, Lee JW, Srikanth R. Edge chipping and flexural resistance of monolithic ceramics. Dent Mater. 2013;29:1201–8.
25. Della Bona A, Kelly JR. The clinical success of all-ceramic restorations. J Am Dent Assoc. 2008;139:8–13.
26. Xu Y, Han J, Lin H, An L. Comparative study of flexural strength test methods on CAD/CAM Y-TZP dental ceramics. Regenerative Biomater. 2015;2(4):239–44.
27. Egilmez F, Ergun G, Cekic-Nagas I. Factors affecting the mechanical behavior of Y-TZP. J Mech Behav Biomed Mater. 2014;37:78–87.
28. Schatz C, Strickstrock M, Roos M, Edelhoff D, Eichberger M, Zylla IM, et al. Influence of specimen preparation and test methods on the flexural strength results of monolithic zirconia materials. Materials. 2016;9(3):180.
29. Guazzato M, Albakry M, Swain MV, Ironside J. Mechanical properties of in-ceram alumina and in-ceram zirconia. Int J Prosthodont. 2002;15:339–46.
30. Lawn BR, Deng Y, Thompson VP. Use of contact testing in the characterization and design of all-ceramic crown like layer structures: a review. J Prosthet Dent. 2001;86:495–510.
31. Pozzobon JL, Wandscher VF, Rippe MP, Valandro LF. Influence of zirconia surface treatments on resin cement bonding and phase transformation. J Adhes Sci Technol. 2017;19(1):7–19.
32. Wong ACH, Tian T, Tsoi JKH, Burrow MF, Matinlinna JP. Aspects of adhesion tests on resin–glass ceramic bonding. Dent Mater. 2017;33(9):1045–55.
33. Şanlı S, Comlekoğlu MD, Comlekoğlu E, Sonugelen M, Pamir T, Darvell BW. Influence of surface treatment on the resin-bonding of zirconia. Dent Mater. 2015;31(6):657–68.
34. Yavuz T, Özyılmaz .ÖY, Dilber E, Tobi ES, Kilic HŞ. Effect of different surface treatments on porcelain-resin bond strength. J Prosthodont. 2017;26(5):446–54.
35. Blatz MB, Sadan A, Kern M. Resin-ceramic bonding: a review of the literature. J Prosthet Dent. 2003;89:268–74.
36. Kosmač T, Oblak C, Jevnikar P, Funduk N, Marion L. The effect of surface grinding and sandblasting on flexural strength and reliability of y-tzp zirconia ceramic. Dent Mater. 1999;15:426–33.
37. Kosmac T, Oblak C, Jevnikar P, Funduk N, Marion L. Strength and reliability of surface treated Y-TZP dental ceramics. J Biomed Mater Res. 2000;53(4):304–13.
38. Bärsch N, Werelius K, Barcikowski S, Liebana F, Stute U, Ostendorf A. Femtosecond laser micro-structuring of hot-isostatically pressed zirconia ceramic. J Laser Appl. 2007;19(2):107–15.

39. Yucel MT, Kilic I, Kilic HS, Gundogdu Y, Okutan Y. Effect of femtosecond laser beam angle and formed shape on surface roughness and shear bond strength between zirconia and resin cement. J Adhes Sci Technol. 2018;32(12):1265–77.
40. Hao L, Lawrence J. Effects of Nd: YAG laser treatment on the wettability characteristics of zirconia-based bioceramics. Opt Laser Eng. 2006;44:803–14.